Coupling Heat Curing and Surface Modification for the Fabrication of High Permselectivity Polyamide Nanofiltration Membranes

Zi-Ming Zhan[a], Yong-Jian Tang[a*], Ka-Ke Zhu[a], Shuang-Mei Xue[b], Chen-Hao Ji[b], Chuyang Y. Tang[c] and Zhen-Liang Xu[a*]

[a] *State Key Laboratory of Chemical Engineering, Membrane Science and Engineering R&D Lab, Chemical Engineering Research Center, School of Chemical Engineering, East China University of Science and Technology, 130 Meilong Road, Shanghai 200237, China*

[b] *Institute for Advanced Study, Shenzhen University, Shenzhen 518060, China*

[c] *Department of Civil Engineering, The University of Hong Kong, Pokfulam HW619B, Hong Kong, China*

Abstract: Surface modification is an efficient post-treatment method to optimize the properties of nanofiltration (NF) membranes. Here, we report a facile surface modification strategy coupling with heat curing for grafting monoethanolamine (MEA), a monomer containing both a primary amine and a primary alcohol group, onto a nascent polyamide NF membrane. With grafting 0.5 wt% MEA at 50 °C, the pure water permeability of the polyamide NF membranes was improved from 7.9 to 19.5 L m^{-2} h^{-1} bar^{-1} due to their enhanced physicochemical property, such as superior hydrophilicity, rough surface morphology, and enlarged membrane pores. Meanwhile, the rejection of Na_2SO_4 remained above 97.5%. More importantly, the optimal membrane modified with 0.5 wt% MEA exhibited a high Na_2SO_4 rejection of 99.1% and a negative NaCl rejection of -20.1% when treating a mixed salt solution containing 2 g/L Na_2SO_4 and 2 g/L NaCl. Our study provides a novel insight for the fabrication of high permselectivity NF membranes via surface modification.

Keywords: membrane fabrication, nanofiltration membrane, surface modification, interfacial polymerization, thin-film composite membrane

* To whom all correspondence should be addressed.

Email: tangyongjian@ecust.edu.cn，chemxuzl@ecust.edu.cn; Tel: 86-21-64253670; Fax: 86-21-64252989.

1. Introduction

Water consumption has been continuously raising worldwide in the last decades due to the rapid population growth and industrial development [1, 2], resulting in a global challenge of water scarcity [3]. To tackle this challenge, numerous studies have been aimed to enlarge freshwater supply through membrane-based water reuse and seawater desalination [4-6], due to its advantages of environmentally friendly, high efficiency, and low energy consumption [7-10]. Particularly, nanofiltration (NF) membranes possess special superiority in the rejection of small organic molecules and selective separation of mono-/di-valent ions, rendering NF a promising technology for desalination and water purification applications [11, 12].

Currently, a thin-film composite (TFC) structure is the most popular design for high-performance NF membranes [13-15]. Such a TFC membrane commonly consists of a polyamide selective layer, a porous interlayer, and a supporting bottom layer [16]. The polyamide selective layer, prepared via interfacial polymerization on a microfiltration/ultrafiltration membrane, has a dominant role in the performance of NF membranes [17, 18]. Many effects have been made to improving water permeance without sacrificing bivalent salts rejection of NF membranes [19]. The main design principles include introducing additional water pathways such as the blend of nanomaterial/aquaporins [20, 21], tuning the physicochemical property of membrane surface such as morphology and hydrophilicity [18, 22, 23], and lowing membrane thickness [24, 25]. Surface modification, which can effectively tailor membrane surface properties, is recognized as a prevailing post-treatment method for enhancing the performance of NF and reverse osmosis (RO) membranes [26]. Jee et al. [27] introduced a hydrophilic agent 3-glycidoxypropyltrimethoxysilane onto the surface of RO membranes via a complex redox reaction. The fouling resistance of the optimized membranes was enhanced. Liu et al. [28] grafted hydrophilic polyvinyl alcohol onto the surface of a polyamide RO membrane by thermally induced radical grafting. The physicochemical property of the PVA-grafted membrane became smoother, less charged, and more hydrophilic. The modified membrane showed improved chlorine

stability and antifouling property, yet a slight decline in water flux. Nevertheless, these existing surface-modified strategies are usually performed after a heat curing process, which involves additional and complex steps. In addition, these strategies by grafting various monomers/polymer generally increase the membrane thickness and thus decrease the water flux to a certain degree [29, 30]. Most importantly, owing to limited active sites (e.g., acyl chloride groups) exposed on the membrane surface after a heat curing process, the improvement in NF performance by these traditional surface modification methods is limited [15, 31].

High salinity wastewater, containing high concentration of Cl^- and SO_4^{2-}, is heavily produced in many industries, such as paper mills, Oil refining, and pharmaceutical factories [32, 33]. Sulfate is an important contaminant that needs to be removed. A high Cl^-/SO_4^{2-} selectivity allows sulfate to be properly removed without facing excessively high trans-membrane osmotic pressure different caused by chloride-based salts [34-36]. Therefore, the separation of Cl^- and SO_4^{2-} by nanofiltration is of great significance for treating high salinity wastewater, which has become a new research hotspot [37, 38]. In order to tune the free volume and surface charge simultaneously for enhanced ion selectivity, hyperbranched polymers, inorganic nanomaterials, and some monomers, that possess internal nanochannels, have been incorporated into the polyamide matrix [39, 40]. Kong et al. [41] introduced three different hyperbranched polyesters into the polyamide selective layer fabricated by the interfacial reaction between trimesoyl chloride and piperazine. The water flux of the optimized membrane was enhanced by 39.8%, which can be ascribed to the reduced crosslinking density and enhanced hydrophilicity of the selective layer. Meanwhile, owing to the enlarged aggregate pores and improved negative charge, the optimized Cl^-/SO_4^{2-} selectivity reached up to 140.

In our previous work, we fabricated a superior NF membrane with a permeability of 10.8 L m^{-2} h^{-1} bar^{-1} via heat curing in neutral water bath [42]. The permeability of the control membrane prepared by heat curing in the air is about 5.3 L m^{-2} h^{-1} bar^{-1}. The results show that this novel heat curing strategy can avoid severe loss in water flux.

Particularly, this strategy provides a possibility for membrane surface modification during the heat curing process. On the basis of our previous work, a simplified and efficient strategy for surface modification has been developed.

In this work, surface modification coupling with heat curing in water was introduced for the preparation of high-performance polyamide NF membranes. Compared with the traditional surface modification methods, this facile strategy not only simplifies the membrane fabrication process but also provides more active sites for grafting, thus more likely tailors the membrane properties. Monoethanolamine (MEA), as a bifunctional molecule containing both a primary amine and primary alcohol, was chosen as the grafting monomer. Owing to the reaction between the amido groups of MEA molecule and the residual acyl chloride groups of the nascent polyamide membrane, MEA molecule can be firmly grafted onto the NF membrane. Meanwhile, the hydroxyl groups of MEA molecule have the potential to enhance the hydrophilicity of the modified NF membrane. The impact of MEA concentration and curing temperature on the membrane physicochemical properties and NF performance was systematically studied. The resultant NF membranes were analyzed by reflectance-fourier transform infrared spectroscopy (ATR-FTIR), energy dispersive X-ray spectrometer (EDX), X-ray photoelectron spectroscopy (XPS), atom force microscopy (AFM), scanning electron microscope (SEM), and zeta potential. This work provides a novel avenue for the fabrication of superior NF membranes.

2. Experimental

2.1. Materials and chemicals

Trimesoyl chloride (TMC, 98%) monomer was provided by Qingdao Benzo Chemical Company. Potassium chloride (KCl, 99.9%) used for zeta potential tests was obtained from Shanghai Titan Scientific Co., Ltd. Monoethanolamine (MEA, >99.0%) was also supplied by Shanghai Titan Scientific Co., Ltd. Other reagents and chemicals were provided by Sinopharm Chemical Reagent Co., Ltd, including piperazine (PIP, GR), n-hexane (AR), and inorganic salts. Polyethersulfone (PES) ultrafiltration

membrane (water flux = 180 L m^{-2} h^{-1} bar^{-1} and MWCO=50,000 Da) was obtained from the Development Center for the Water Treatment Technology.

2.2. Fabrication of control and modified polyamide NF membranes

The desired membranes were prepared by typical interfacial polymerization (Fig. 1). The PES membrane was soaked in deionized (DI) water for 12 hours before using it. The organic phase solution dissolving 0.15 g TMC monomer in 100 ml n-hexane and the aqueous phase solution dissolving 1 g PIP monomer in 100 ml deionized water were prepared. A series of water bath solutions comprising a certain amount of MEA monomer were prepared for heat curing and surface modification. First, the PES membrane was firmly clamped between two home-made molds. The aqueous solution was carefully tipped onto the PES membrane for 3 min [42]. After that, the residual aqueous solution was removed and the visible waterdrop was dislodged using an air knife. Subsequently, the organic solution was tipped on the soaked membrane for 1 min. Finally, the nascent membrane was immersed in a curing solution comprising 0-1 wt% MEA. This process coupling heat curing and surface modification was lasted for 5 min to fabricate the desired polyamide NF membranes. The obtained NF membranes were kept into DI water. The resulting membranes modified by 0, 0.1, 0.5, and 1 wt% MEA solution under 50 ℃ (which was the optimal temperature according to the supporting information) were denoted as M0, M1, M2, and M3, respectively. In addition, a part of resulting membranes was modified by 0.5 wt% MEA solutions at 2, 25, 50, and 80 °C, respectively.

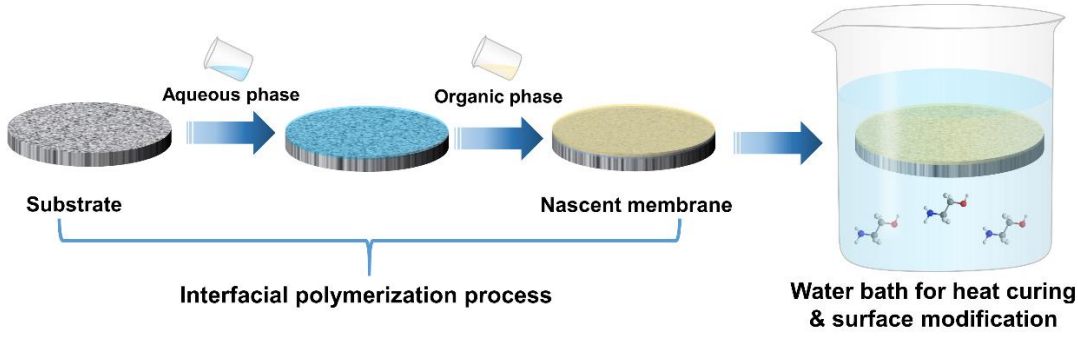

Fig. 1. Schematic illustration of fabricating polyamide NF membranes via coupling heat curing and surface modification

2.3. Membrane characterization

X-ray photoelectron spectroscopy (XPS, Thermo Fisher Scientific, USA) and attenuated total reflectance-fourier transform infrared spectroscopy (ATR-FTIR, NEXUS 670, Thermo Nicolet, USA) were adopted to characterize the surface chemical composition of the obtained TFC NF membranes. Scanning electron microscope (SEM, FEI, USA) was utilized to test the surface and cross-sectional morphology of the selective layer. Energy Dispersive X-ray spectrometer (EDX, Hitachi S3400 N, Japan) was used to characterize the distribution of element N within the polyamide selective layer, and each sample was tested under a voltage of 10 kV for 30 scans. Atom force microscopy (AFM, NanoScope IIIa, Veeco, USA) was employed to measure the surface roughness of NF membranes. Zeta potential was tested at pH 7 using 1 mM KCl by a potentiometric analyzer (SurPASS 3, Anton Paar, Austria). A water contact angle meter (JC2000D, Shanghai ZhongCheng Digital Technology Apparatus Co., Ltd., China) was employed to estimate the hydrophilicity of the NF membranes. The PEG concentration was tested by a total organic carbon analyzer (TOC-L $_{CPH/CPN}$, SHIMADZU, Japan). The Cl^- and SO_4^{2-} concentration of the mixed salts were tested by ion chromatography (ThermoFisher, ICS-5000, USA).

2.4. Nanofiltration performance tests

A home-made cross-flow device with a filtration area of 28.3 cm^2 was used to test the NF performance (Fig. 2). Various inorganic salt solutions were prepared to evaluate the separation performance. Unless otherwise specified, the salt concentration was 2000 ppm. All the tests were carried out under 5 bar and operated for at least 30 min before collecting experimental data. To avoid artificial error, three independently fabricated membranes were tested for each membrane type. The concentration of the salt solution is positively related to its conductivity that was tested by a conductivity meter (DDS-307A, Shanghai Neici Instrument Company, China). The inorganic salt rejection (R) is obtained by the following formula:

$$R = (1 - \frac{\sigma_p}{\sigma_f}) \times 100\% \quad (1)$$

where σ_p and σ_f represent the conductivity of the permeance and feed solution,

respectively. The membrane permeability is obtained by the following equation:

$$P = \frac{V}{A \times t \times (\Delta p - \Delta \pi)} \quad (2)$$

Where P (L m^{-2} h^{-1} bar^{-1}) represents the membrane permeability, V (L) represents the permeated solution volume, t (h) represents the testing time, A (m^{-2}) represents the filtration area, Δp (bar) represents the operating pressure and $\Delta \pi$ (bar) represents the osmotic pressure difference. The selectivity of Cl^-/SO_4^{2-} is obtained by the following equation:

$$S_{Cl^-/SO_4^{2-}} = (100 - R_{Cl^-})/(100 - R_{SO_4^{2-}}) \quad (3)$$

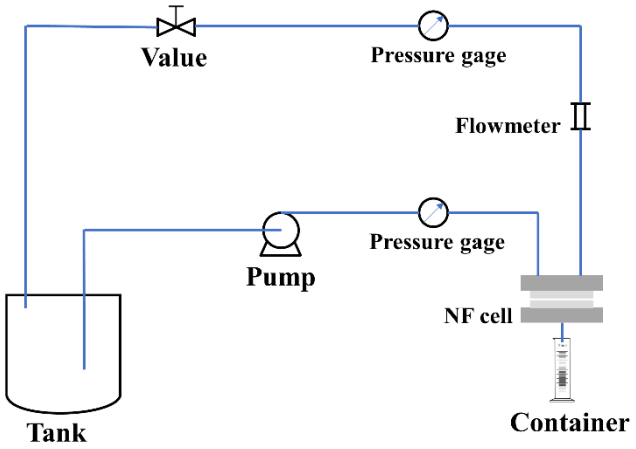

Fig. 2. Schematic diagram of the cross-flow nanofiltration test system

3. Results and discussion

3.1 Chemical composition and structure

In order to verify that MEA was successfully grafted onto polyamide selective layer, IR, EDS, and XPS were employed to explore the variation of chemical composition and structure of the membrane surface. The peak at 3450 cm^{-1} attributing to the O-H and N-H stretching vibration is observed by all the obtained membranes (Fig. 3a). According to the report of Tang et al. [43], the tertiary amide group reacted by PIP and TMC owns the characterized peak at 1630 cm^{-1}, while the secondary amide group formed by m-phenylenediamine and TMC possesses the typical peak at 1663 cm^{-1} (representing the amide I band) and 1541 cm^{-1} (representing the amide II band). As shown in Fig. 3a, M0 owns a significant peak at 1630 cm^{-1}, demonstrating the generation of the poly(piperazine-amide) selective layer. After the surface modification

of MEA, M1, M2, and M3 possess an apparent peak at 1657 cm^{-1}, which is assigned to the C=O stretching vibration of a -CO-NH- group formed by MEA and TMC. Compared with the typical peak at 1663 cm^{-1} (amide I band), it has a slight deviation. This phenomenon could be caused by the existence of the tertiary amide group (1630 cm^{-1}) reacted by PIP and TMC in the modified membrane. However, the amide II band with a peak at 1541 cm^{-1} of M1-M4 is not obvious. This may be ascribed to the limited grafting of MEA resulted in the week signal of N-H in-plane bending. Thus, we would further study the chemical structure of the selective layer based on EDX and XPS analysis.

EDX mapping images were employed to analyze the variation of element N within the polyamide selective layer. As shown in Fig. 3b and Fig. 3c, yellow spots based on a black background exhibit the distribution of element N within the selective layer. Compared with M0, the significantly increased content of element N in M2 verifies that MEA was successfully reacted with the acyl chloride group that is exposed on the membrane surface. Furthermore, the uniform distribution of element N demonstrates that MEA was homogenously grafted onto the NF membrane surface, confirming water bath treatment as a feasible strategy for surface modification.

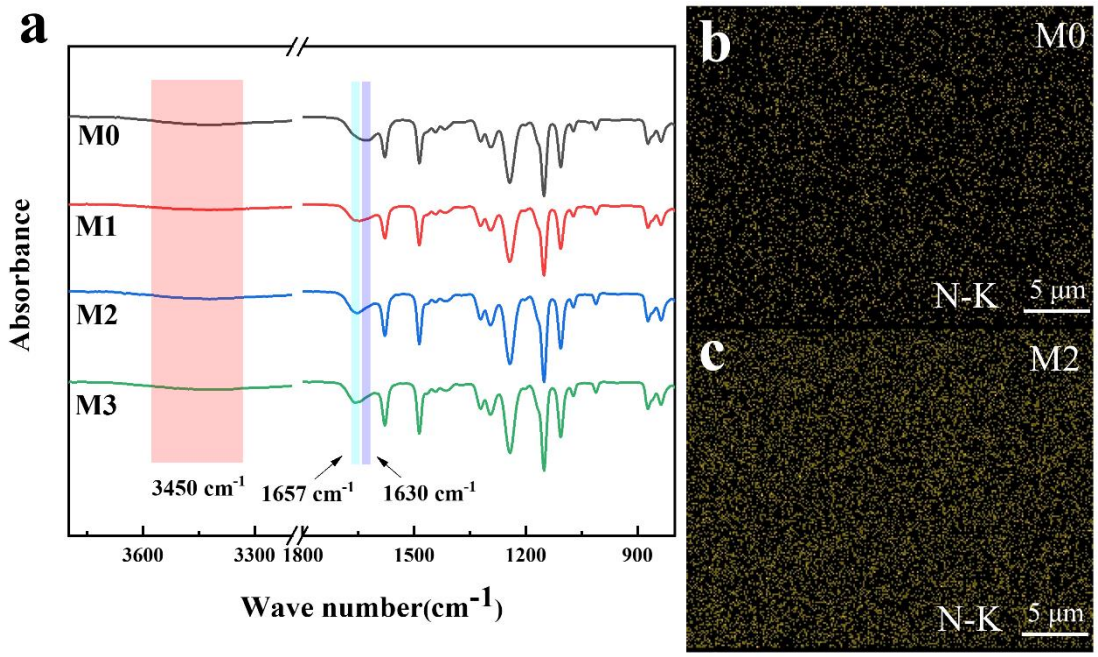

Fig. 3. (a) IR spectra of the obtained NF membranes; (b) (c) EDX mapping images of M0 and M2 membrane

Further detailed analysis of the chemical structure of the selective layer was conducted through XPS spectra (Fig. 4). Three main peaks around binding energy of 284, 399, and 532 eV, corresponding to C1s, N1s, and O1s, respectively, are observed. With the modification by MEA, the nitrogen content is increased from 11.5% (M0) to 13.3% (M2), which is consistent with the EDX results. In addition, high-resolution XPS spectra were utilized to further analyze the detailed chemistry environment of C atoms. The peaks centered around 285.0, 286.3, 288.2, and 288.8 eV are assigned to C-C or C-H, C-N, O=C-N, and O=C-O, respectively [25]. There are significant changes in peak area, indicating a transformation in the chemical structure of the membrane surface. Owning to the amide bonds generated by grafting MEA molecule, it is hard to precisely calculate the cross-linking density of the M2 membrane based on the XPS results. As shown in Fig. 4c and 4d, the O=C-N contents of M0 and M2 membrane are 10.6% and 9.6%, respectively. Though the introduction of amide bonds generated by grafting MEA molecule, the O=C-N content of M2 membrane is still lower than that of M0 membrane, indicating that the polypiperazine-amide cross-linking density of M2 membrane is reduced. Since the pH value of the 0.5 wt% MEA solution was 11.2, this abnormal phenomenon may be ascribed to the hydrolysis of amide bond under alkaline solution [42, 44]. In order to further verify the grafting of MEA molecule, the O1s narrow spectra was analyzed. The peaks of O=C-N, O-H, and O=C-O are centered around 532.0, 532.8, and 533.5 eV, respectively [25, 45]. Compared with the O1s narrow spectra of M0 membrane, a new O-H peak was detected for the M2 membrane confirming the successful grafting of MEA onto the membrane surface. The effect of the alkalinity of MEA solution on grafting degree has also been studied. The detailed discussions have been provided in the supporting information (Fig. S5).

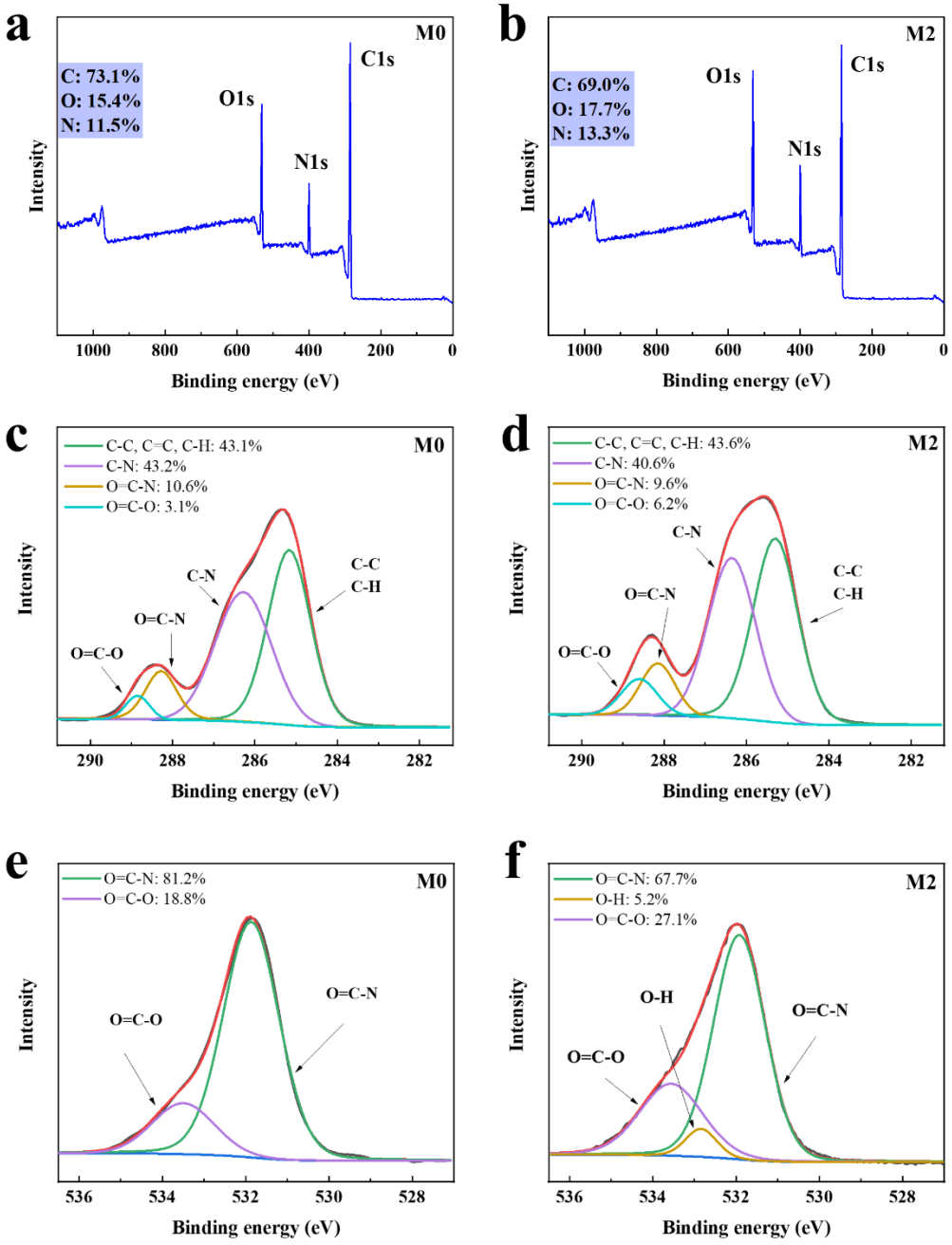

Fig. 4. (a, b) XPS spectra, (c, d) C1s narrow spectra, and (e, f) O1s narrow spectra of M0 and M2 membrane.

3.2 Surface morphology

The surface and cross-section morphologies of the obtained NF membranes are presented in Fig. 5. A nodular morphology, which is typical for polyamide membranes synthesized by the polycondensation between PIP and TMC [22, 46], are observed for all the membranes. According to the SEM surface images, a relatively smoother surface morphology can be seen on M0. With the increase in the MEA concentration, the

nodular morphology becomes grainier and the obvious gully can be observed on M3. The pH value of 0.5 wt% MEA solution was 11.2 at 50 °C. The change of membrane morphology is may not only caused by MEA grafting, but also caused by the hydrolysis of some vulnerable amide bonds under alkaline condition. To verify that, we have provided the SEM image with 100, 000 times magnifications of the membrane treated by NaOH solution (without MEA) under pH 11.2. As shown in Fig. S4, the surface morphology of M0 is relatively smoother, and some gullies appear on the surface of the membrane treated by NaOH solution. With the grafting of MEA molecule, the gully and graininess of the M2 membrane surface is more pronounced. Therefore, the obvious change in membrane morphology can be attributed to the combined effect of the MEA grafting and the hydrolysis of some vulnerable amide bonds. AFM images were employed to further reveal the membrane surface morphology. The roughness values of the obtained NF membranes follow the order of M3>M2>M1>M0, indicating the high consistency between AFM and SEM results. The thickness of the separation layer was tested based on SEM cross-section images. There is no major difference in thickness among these obtained membranes. In the current study, the creation of a rougher morphology without a major increase in the thickness of the rejection layer by this grafting strategy could be beneficial for enhancing water permeability [30, 47].

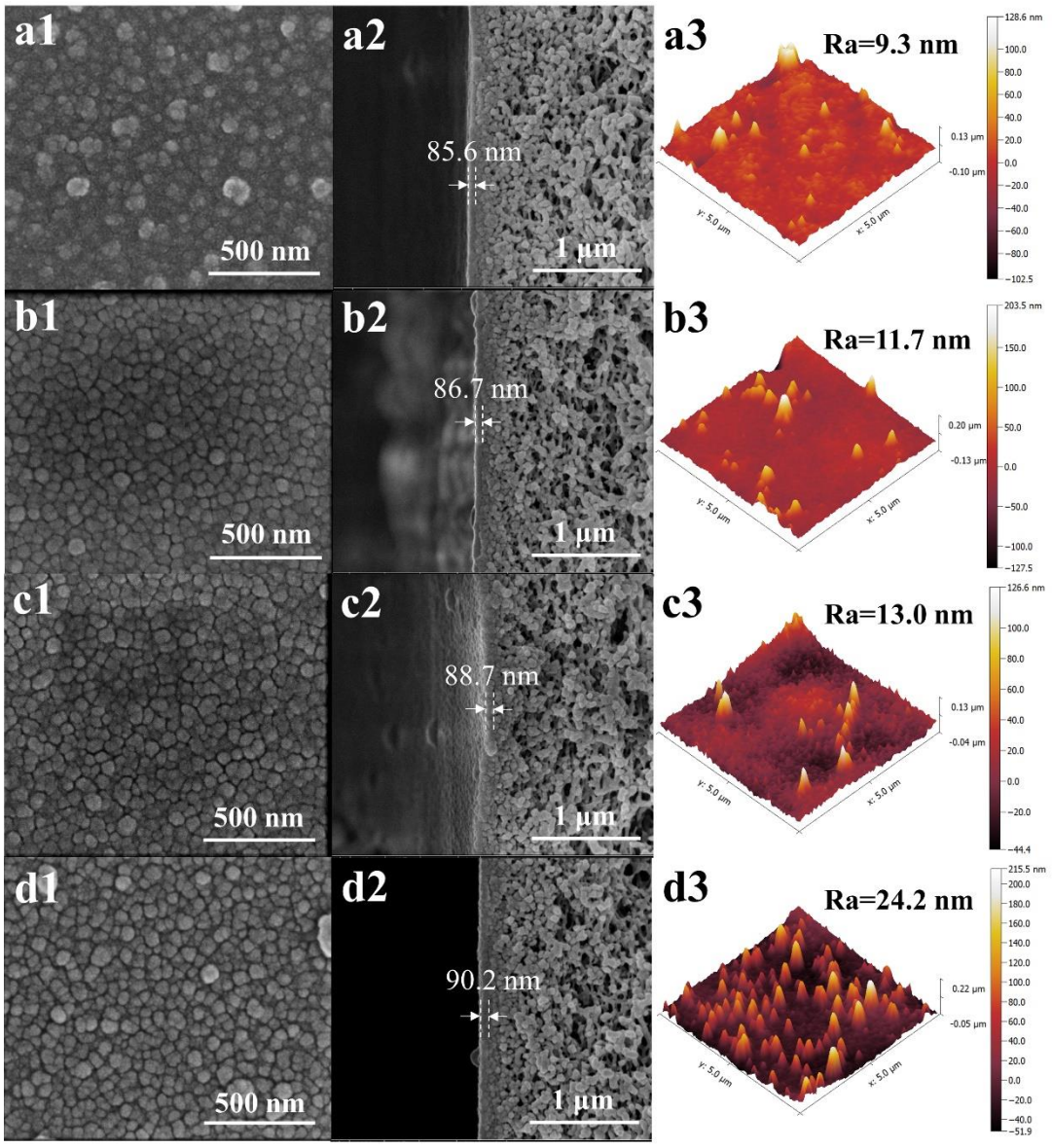

Fig. 5. The SEM surface morphology, SEM cross-section morphology, and AFM surface images of (a1-a3) M0 membrane; (b1-b3) M1 membrane; (c1-c3) M2 membrane; (d1-d3) M3 membrane

3.3 Surface charge and hydrophilicity

As shown in Fig. 6, the M3 membrane modified with 1 wt% MEA solution exhibited more negative charge. This could be attributed to the partial hydrolysis of some vulnerable amide bonds under alkaline conditions, thus generating more negatively charged carboxyl groups. Hydrophilicity has a dominant role in the NF performance of the obtained membranes and it is mainly characterized through the dynamic water contact angle. A low water contact angle normally means good hydrophilicity and vice versa. The dynamic water contact angle was tested every 2 s

within 40 s. As shown in Fig. 7, M0 membrane exhibits a dynamic water contact angle from 46.1° (at 0 s) to 35.0° (at 40 s). With increasing the MEA concentration for surface modification, the modified membranes show better hydrophilicity. For example, with a MEA concentration of 1 wt%, the contact angle is greatly reduced to 12.0° at 40 s for M3. This could be primarily ascribed to the introduction of hydroxyl groups by grafting the MEA molecule, which was verified through XPS results.

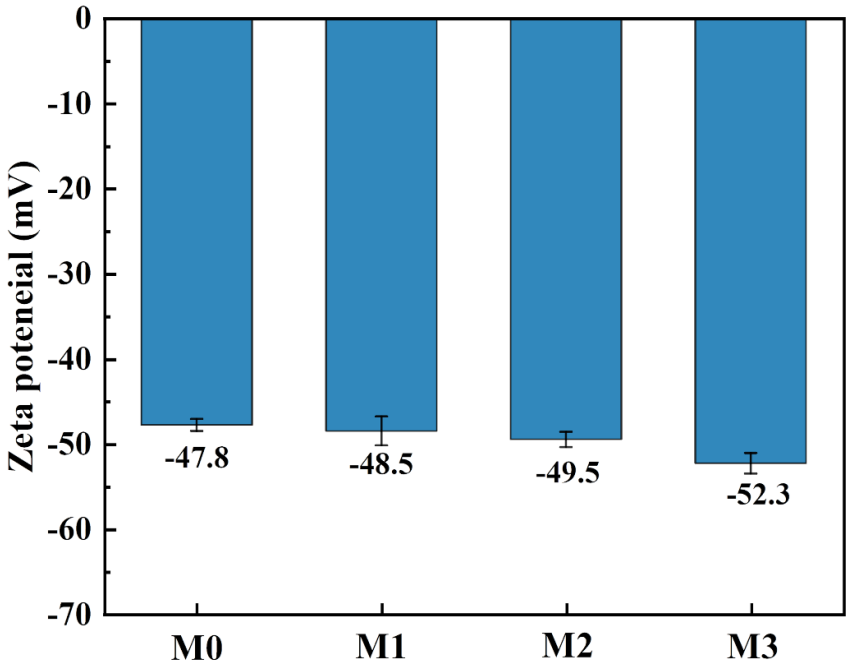

Fig. 6. Zeta potential of the obtained nanofiltration membranes

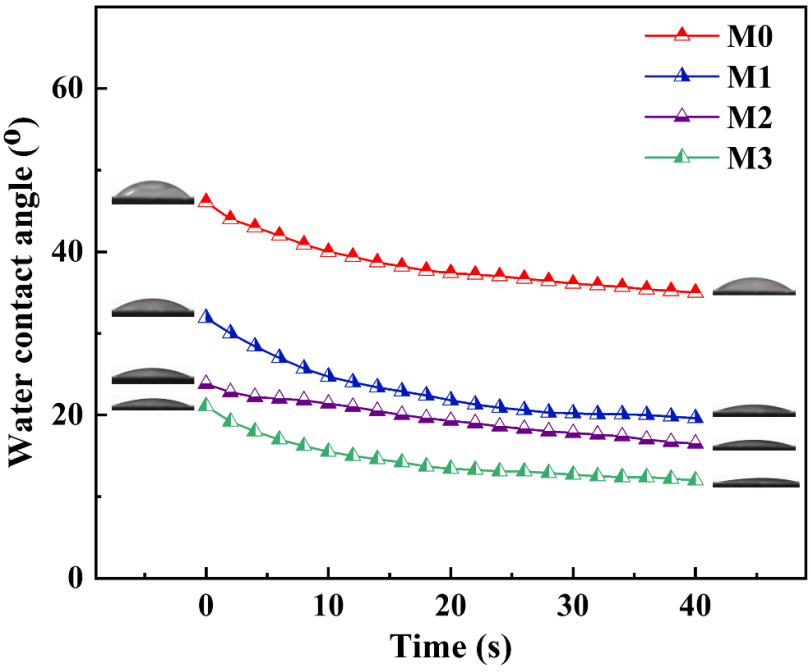

Fig. 7. The dynamic water contact angle of the obtained NF membranes

3.4 MWCO

The molecular weight cutoff (MWCO) was measured using a series of PEG solutions, each containing 0.3 g/L PEG with an average molecular weight of 200, 300, 400, or 600 Da, and the molecular weight of PEG which having 90% rejection is defined as the MWCO of the membrane. As shown in Fig. 8, the MWCOs of M0, M1, and M2 membranes are marginally increased as the MEA concentration increased from 0 wt% to 0.5 wt%, revealing a slight increase in pore size. When further improving MEA concentration to 1 wt%, the resulted M3 membrane has a much greater MWCO of 268 Da. As mentioned above, this may be caused by the partial hydrolysis of some vulnerable amide bonds. We have chosen the 5-carbon surge xylose and the 6-carbon surge glucose to test the rejection of monosaccharides. The concentration of feed solution was 0.3 g/L. The results are shown in Table S4. The glucose rejection of M0 and M2 membrane is 92.8% and 82.9%, respectively.

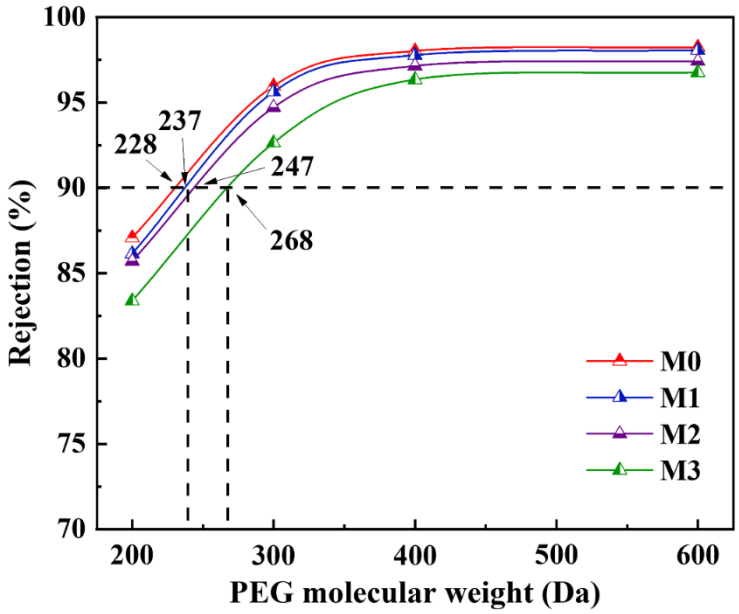

Fig. 8. The MWCO of the obtained NF membranes

3.5 Nanofiltration performance

The impact of MEA concentration on the NF performance of the resulted membranes was studied and the results are presented in Fig. 9a. PWP improved with the increase of MEA concentration from 0 wt% to 0.5 wt%, while the Na_2SO_4 rejection remained above 97.5%. However, when the MEA concentration further increased to

1wt%, Na_2SO_4 rejection rapidly reduced to 84.3%. The M2 membrane, which was modified by 0.5wt% MEA solution, showed the most promising combination of permeability and Na_2SO_4 rejection. Compared with the control membrane, the PWP of the M2 membrane sharply increased from 7.9 to 19.5 L m^{-2} h^{-1} bar^{-1}. As mentioned above, with the rise of MEA concentration, the enhanced hydrophilicity and slightly enlarged pore size may result in the increase of permeability. When the MEA concentration is above 0.5 wt%, the increased alkaline condition of the MEA solution may cause the hydrolysis of some nascent amide bonds, thus enlarged the membrane pore size and decreased Na_2SO_4 rejection of M3.

The effect of curing temperature on the membrane performance was also investigated. To minimize the effect of heat curing, the MEA solution temperature was down to 2°C to merely graft MEA molecule without heat curing. As shown in Table S1, the results showed that the membrane optimized at low temperature is hard to reach the optimal performance due to the reduced MEA reactively (Fig. S1-S3). As shown in Table S2, with the increase in curing temperature, the PWP of the prepared membrane improved. However, the membrane cured at 80 °C owned a loss in Na_2SO_4 rejection. This phenomenon was mainly due to the increased partial hydrolysis of some vulnerable amide bonds caused by the alkalinity of MEA under high curing temperature. Therefore, 50°C was the optimal temperature.

The separation ability to various inorganic salts of the optimal NF membrane (M2) was systematically studied (Fig. 9b). The salt rejection to Na_2SO_4, $MgSO_4$, $MgCl_2$, and NaCl was 98.9%, 97.9%, 88.3%, and 17.6%, respectively, using feed solution containing a single type of salt for each rejection test. The corresponding permeability was 12.3, 13.8, 11.3, and 16.3 L m^{-2} h^{-1} bar^{-1}, respectively. The high rejection of Na_2SO_4 and relatively low rejection of $MgCl_2$ indicate that the M2 membrane is a typical negatively charged membrane. It is worth noting that the rejection of NaCl was as low as 17.6%. This phenomenon could be attributed to the enlarged pore size, indicating this surface modification strategy could precisely tailor the membrane pore size for monovalent ions separation.

In practical applications, the stability of the NF membrane is a crucial criterion. Hence, the stability of M2 membrane was also studied. A series of Na_2SO_4 feed solutions with a concentration from 1 g/L to 6 g/L were prepared to evaluate the separation performance under various feed concentration. It is displayed in Fig. 9c that the permeability slightly declined with the increased feed concentration, which could be due to the viscosity variation in feed solution [48, 49]. Nevertheless, the salt rejection remained almost unchanged, verifying that the obtained membrane had a good tolerance to feed concentration. In addition, a continuous nanofiltration testing at 5 bar for 10 days was carried out to assess the stability of the surface modified NF membrane in permeability and Na_2SO_4 rejection. As shown in Fig. 9d, both permeability and Na_2SO_4 rejection maintained essentially constant, demonstrating that the modified NF membrane owns great stability for NF performance.

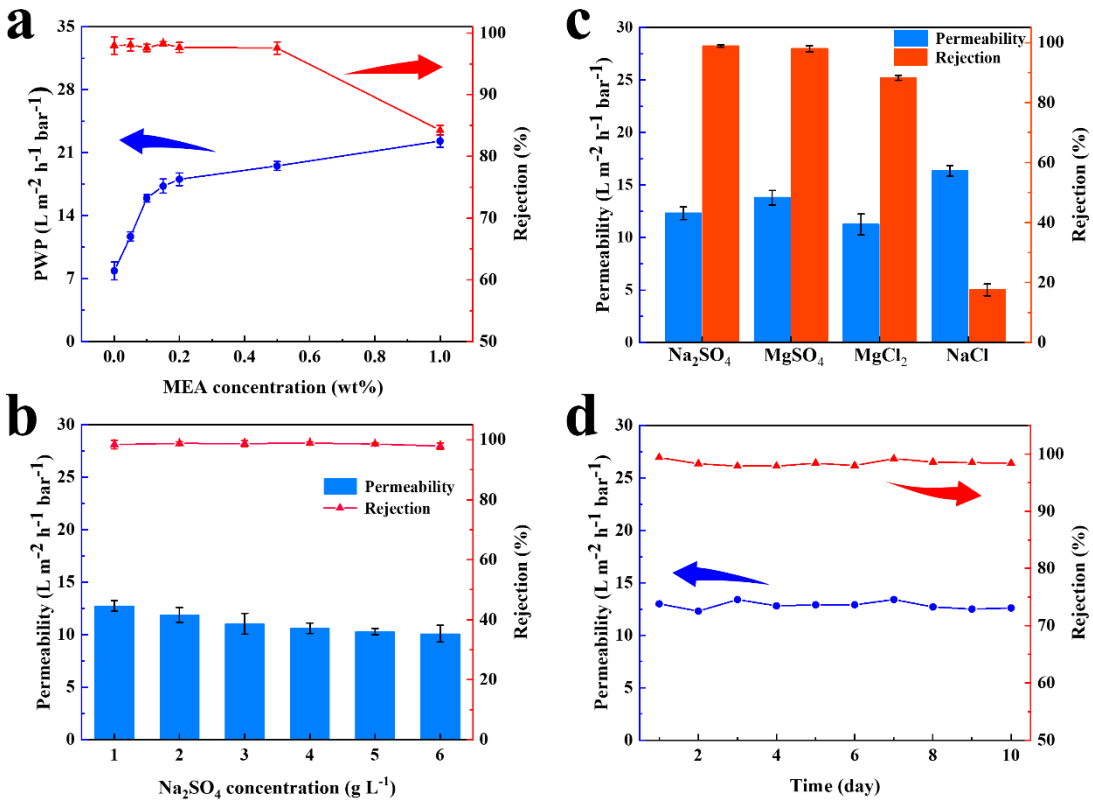

Fig. 9. NF performance and stability of the obtained NF membranes: (a) the effect of MEA concentration on membrane permeability and rejection; (b) the permeability and various salt rejection of the optimal NF membrane (M2) under various inorganic salts; (c) the impact of Na_2SO_4 concentration on permeability and rejection of M2 membrane; (d) the 10-day stability test of M2 membrane (Unless otherwise specified, the feed solution contained a single type of salt at 2000 ppm, and the running pressure was 5 bar.)

As mentioned above, the M2 membrane exhibited a low rejection of NaCl while a high rejection of Na_2SO_4. In order to further investigate the Cl^-/SO_4^{2-} selectivity of the obtained NF membranes, solutions containing mixed salts (either 1 g/L NaCl plus 1 g/L Na_2SO_4 or 2 g/L NaCl plus 2 g/L Na_2SO_4) was employed for the separation performance test (Table 1). Compared with the M0 membrane, the M2 membrane had a higher SO_4^{2-} rejection, which could be attributed to the slightly enhanced negatively charged selective layer. Nevertheless, the Cl^- rejection of the M2 membrane was lower than that of the M0 membrane, which could be ascribed to the relatively enlarged membrane pore size. Therefore, the M2 membrane exhibited a better Cl^-/SO_4^{2-} selectivity. Interesting, negative rejections of NaCl were observed for the M2 membrane. Such negative NaCl rejections have also been reported in other literature as well [50-52]. In the NaCl/Na_2SO_4 mixed solution, the Na^+ concentration was far greater than the Cl^- concentration. For the negatively charged NF membranes, sodium is easier to pass through the membrane compared with anion ions due to the electrostatic attraction effect. Owning to the higher exclusion of SO_4^{2-}, Cl^- would preferentially pass through the membrane as the counter ion of Na^+ to keep the electroneutrality [51, 53]. Consequently, the Cl^- concentration in permeate solution is higher than that in feed solution, causing its negative rejection. In addition, with the increased salt concentration of the feed solution, the Cl^-/SO_4^{2-} selectivity was significantly strengthened. Such a high ions selectivity is beneficial for monovalent ions to pass through the membrane while maintaining a high rejection of multivalent ions, indicating that the modified NF membrane could be promising for application in seawater pretreatment, water softening, and wastewater decontamination. In addition, the permeability and Cl^-/SO_4^{2-} selectivity of NF membranes reported in literatures are summarized in Fig. 10 [39, 41, 52, 54-57]. It can be seen that the M2 membrane had an outstanding Cl^-/SO_4^{2-} selectivity while maintaining a highly competitive permeability.

Table 1

The Cl^-/SO_4^{2-} selectivity of M0 and M2 membrane

membrane	Feed solution	Rejection rate (%)		$S_{Cl^-/SO_4^{2-}}$
		Cl^-	SO_4^{2-}	
M0	1.0 g/L NaCl and 1.0 g/L Na_2SO_4	26.3	96.7	22.3
	2.0 g/L NaCl and 2.0 g/L Na_2SO_4	10.3	96.8	28.0
M2	1.0 g/L NaCl and 1.0 g/L Na_2SO_4	-7.9	98.9	98.1
	2.0 g/L NaCl and 2.0 g/L Na_2SO_4	-20.1	99.1	133.4

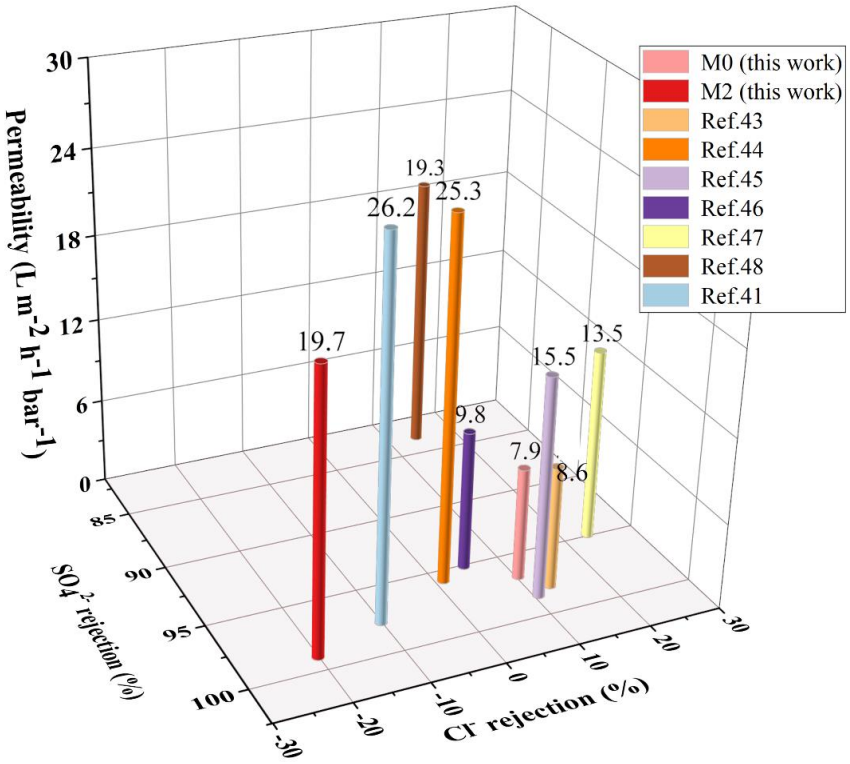

Fig. 10. Comparison with other highly permeable and selective NF membranes reported in literatures

4. Conclusions

In this work, we prepared highly permeable and selective polyamide NF membranes via coupled heat curing and surface modification. MEA molecules were grafted onto the nascent polyamide membrane during the heat curing process, taking advantage of the reactive acyl groups to form amide bonds with MEA. The optimal NF membrane exhibited outstanding permeability of 19.5 L m^{-2} h^{-1} bar^{-1}, and had a greatly enhanced selectivity for mono-/di-valent salt separation. This study provides a novel insight and pathway for the preparation of high-performance polyamide membranes via

surface modification.

Acknowledgement

The authors greatly acknowledge the funding supported by National Natural Science Foundation of China (21808060) and Fundamental Research Funds for the Central Universities (222201814009, JKA012011001 and JKA012011017).

REFERENCES

[1] M. Elimelech, W.A. Phillip, The future of seawater desalination: energy, technology, and the environment, Science 333 (2011) 712-717.

[2] Y. Wada, L. Van Beek, D. Viviroli, H.H. Dürr, R. Weingartner, M.F. Bierkens, Global monthly water stress: 2. Water demand and severity of water stress, Water Resour. Res. 47 (2011) W07518.

[3] M.M. Mekonnen, A.Y. Hoekstra, Four billion people facing severe water scarcity, Sci. Adv. 2 (2016) e1500323.

[4] J. Ma, M. Xia, S. Zhu, F. Wang, A new alendronate doped HAP nanomaterial for Pb^{2+}, Cu^{2+} and Cd^{2+} effect absorption, J. Hazard. Mater. 400 (2020) 123143.

[5] S. Mondal, S.R. Wickramasinghe, Produced water treatment by nanofiltration and reverse osmosis membranes, J. Membr. Sci. 322 (2008) 162-170.

[6] C.Y. Tang, Z. Yang, H. Guo, J.J. Wen, L.D. Nghiem, E. Cornelissen, Potable Water Reuse through Advanced Membrane Technology, Environ. Sci. Technol. 52 (2018) 10215-10223.

[7] A.G. Fane, R. Wang, M.X. Hu, Synthetic membranes for water purification: status and future, Angew. Chem. Int. Ed. 54 (2015) 3368-3386.

[8] J.R. Werber, C.O. Osuji, M. Elimelech, Materials for next-generation desalination and water purification membranes, Nat. Rev. Mater. 1 (2016) 1-15.

[9] B. McVerry, M. Anderson, N. He, H. Kweon, C.H. Ji, S.M. Xue, E. Rao, C. Lee, C.W. Lin, D.Y. Chen, D. Jun, G. Sant, R.B. Kaner, Next-Generation Asymmetric Membranes Using Thin-Film Liftoff, Nano Lett. 19 (2019) 5036-5043.

[10] X. Zhang, F.Y. Cheng, H.Z. Zhang, Z.L. Xu, S.M. Xue, X.H. Ma, X.R. Xu, In-situ synthetic modified metal-organic framework (MZIF-8) as an interlayer of the composite membranes for ethanol dehydration, J. Membr. Sci. 601 (2020) 117916.

[11] A.W. Mohammad, Y.H. Teow, W.L. Ang, Y.T. Chung, D.L. Oatley-Radcliffe, N. Hilal, Nanofiltration membranes review: Recent advances and future prospects, Desalination 356 (2015) 226-254.

[12] S. Xue, C. Ji, M.D. Kowal, J.C. Molas, C.-W. Lin, B.T. McVerry, C.L. Turner, W.H. Mak, M. Anderson, M. Muni, E.M.V. Hoek, Z.-L. Xu, R.B. Kaner, Nanostructured Graphene Oxide Composite Membranes with Ultrapermeability and Mechanical Robustness, Nano Lett. (2020) 2209-2218.

[13] S. Bano, A. Mahmood, S.-J. Kim, K.-H. Lee, Graphene oxide modified polyamide nanofiltration membrane with improved flux and antifouling properties, J. Mater. Chem. A. 3 (2015) 2065-2071.

[14] Z. Yang, H. Guo, C.Y.Y. Tang, The upper bound of thin-film composite (TFC) polyamide membranes for desalination, J. Membr. Sci. 590 (2019) 117297.

[15] G.R. Xu, J.N. Wang, C.J. Li, Strategies for improving the performance of the polyamide thin film composite (PA-TFC) reverse osmosis (RO) membranes: Surface modifications and nanoparticles incorporations, Desalination 328 (2013) 83-100.

[16] M.C. Porter, Handbook of industrial membrane technology, (1989).

[17] M.J. Raaijmakers, N.E. Benes, Current trends in interfacial polymerization chemistry, Prog. Polym. Sci. 63 (2016) 86-142.

[18] Z. Tan, S. Chen, X. Peng, L. Zhang, C. Gao, Polyamide membranes with nanoscale Turing structures for water purification, Science 360 (2018) 518-521.

[19] W.J. Lau, G. Stephen, T. Matsuura, ., D. Emadzadeh, ., C. J Paul, A.F. Ismail, A review on polyamide thin film nanocomposite (TFN) membranes: History, applications, challenges and approaches, Water Res.

80 (2015) 306-324.
[20] C. Ji, S. Xue, Y.-J. Tang, X.-H. Ma, Z.-L. Xu, Polyamide Membranes with Net-Like Nanostructures Induced by Different Charged MOFs for Elevated Nanofiltration, ACS Appl. Polym. Mater. 2 (2020) 585-593.
[21] Y.L. Ji, W.J. Qian, Y.W. Yu, Q.F. An, L.F. Liu, Y. Zhou, C.J. Gao, Recent developments in nanofiltration membranes based on nanomaterials, Chin. J. Chem. Eng. 25 (2017) 1639-1652.
[22] Z.-M. Zhan, Z.-L. Xu, K.-K. Zhu, Y.-J. Tang, How to understand the effects of heat curing conditions on the morphology and performance of polypiperazine-amide NF membrane, J. Membr. Sci. 597 (2020) 117640.
[23] W. Shang, F. Sun, W. Jia, J. Guo, S. Yin, P.W. Wong, A.K. An, High-performance nanofiltration membrane structured with enhanced stripe nano-morphology, J. Membr. Sci. 600 (2020) 117852.
[24] J. Yuan, M. Wu, H. Wu, Y. Liu, X. You, R. Zhang, Y. Su, H. Yang, J. Shen, Z. Jiang, Covalent organic framework-modulated interfacial polymerization for ultrathin desalination membranes, J. Mater. Chem. A. 7 (2019) 25641-25649.
[25] S. Karan, Z. Jiang, A.G. Livingston, Sub-10 nm polyamide nanofilms with ultrafast solvent transport for molecular separation, Science 348 (2015) 1347-1351.
[26] D. Ankoliya, B. Mehta, H. Raval, Advances in surface modification techniques of reverse osmosis membrane over the years, Sep. Sci. Technol. (Philadelphia) 54 (2019) 293-310.
[27] K.Y. Jee, D.H. Shin, Y.T. Lee, Surface modification of polyamide RO membrane for improved fouling resistance, Desalination 394 (2016) 131-137.
[28] M. Liu, Q. Chen, L. Wang, S. Yu, C. Gao, Improving fouling resistance and chlorine stability of aromatic polyamide thin-film composite RO membrane by surface grafting of polyvinyl alcohol (PVA), Desalination 367 (2015) 11-20.
[29] Y.T. Hu, K. Lu, F. Yan, Y.L. Shi, P.P. Yu, S.C. Yu, S.H. Li, C.J. Gao, Enhancing the performance of aromatic polyamide reverse osmosis membrane by surface modification via covalent attachment of polyvinyl alcohol (PVA), J. Membr. Sci. 501 (2016) 209-219.
[30] M. Asadollahi, D. Bastani, S.A. Musavi, Enhancement of surface properties and performance of reverse osmosis membranes after surface modification: A review, Desalination 420 (2017) 330-383.
[31] R.R. Choudhury, J.M. Gohil, S. Mohanty, S.K. Nayak, Antifouling, fouling release and antimicrobial materials for surface modification of reverse osmosis and nanofiltration membranes, J. Mater. Chem. A. 6 (2018) 313-333.
[32] M. Pernetti, L. Di Palma, Experimental evaluation of inhibition effects of saline wastewater on activated sludge, Environ. Technol. 26 (2005) 695-703.
[33] O. Lefebvre, R. Moletta, Treatment of organic pollution in industrial saline wastewater: a literature review, Water Res. 40 (2006) 3671-3682.
[34] Z.-Q. Yan, L.-M. Zeng, Q. Li, T.-Y. Liu, H. Matsuyama, X.-L. Wang, Selective separation of chloride and sulfate by nanofiltration for high saline wastewater recycling, Separ. Purif. Technol. 166 (2016) 135-141.
[35] A. Pérez-González, R. Ibáñez, P. Gómez, A.M. Urtiaga, I. Ortiz, J.A. Irabien, Nanofiltration separation of polyvalent and monovalent anions in desalination brines, J. Membr. Sci. 473 (2015) 16-27.
[36] Z. Yang, P.-F. Sun, X. Li, B. Gan, L. Wang, X. Song, H.-D. Park, C.Y. Tang, A Critical Review on Thin-Film Nanocomposite Membranes with Interlayered Structure: Mechanisms, Recent Developments, and Environmental Applications, Environ. Sci. Technol. (2020).
[37] M. Ahmad, C. Tang, L. Yang, A. Yaroshchuk, M.L. Bruening, Layer-by-layer modification of

aliphatic polyamide anion-exchange membranes to increase Cl^-/SO_4^{2-} selectivity, J. Membr. Sci. 578 (2019) 209-219.
[38] P. Xu, W. Wang, X. Qian, H. Wang, C. Guo, N. Li, Z. Xu, K. Teng, Z. Wang, Positive charged PEI-TMC composite nanofiltration membrane for separation of Li^+ and Mg^{2+} from brine with high Mg^{2+}/Li^+ ratio, Desalination 449 (2019) 57-68.
[39] Y.-J. Tang, B.-J. Shen, B.-Q. Huang, Z.-M. Zhan, Z.-L. Xu, High permselectivity thin-film composite nanofiltration membranes with 3D microstructure fabricated by incorporation of beta cyclodextrin, Separ. Purif. Technol. 227 (2019) 115718.
[40] Y.L. Liu, X.M. Wang, H.W. Yang, Y.F.F. Xie, X. Huang, Preparation of nanofiltration membranes for high rejection of organic micropollutants and low rejection of divalent cations, J. Membr. Sci. 572 (2019) 152-160.
[41] X. Kong, Z.L. Qiu, C.E. Lin, Y.Z. Song, B.K. Zhu, L.P. Zhu, X.Z. Wei, High permselectivity hyperbranched polyester/polyamide ultrathin films with nanoscale heterogeneity, J. Mater. Chem. A. 5 (2017) 7876-7884.
[42] Z.M. Zhan, Z.L. Xu, K.K. Zhu, S.M. Xue, C.H. Ji, B.Q. Huang, C.Y. Tang, Y.J. Tang, Superior nanofiltration membranes with gradient cross-linked selective layer fabricated via controlled hydrolysis, J. Membr. Sci. 604 (2020) 118067.
[43] C.Y.Y. Tang, Y.N. Kwon, J.O. Leckie, Effect of membrane chemistry and coating layer on physiochemical properties of thin film composite polyamide RO and NF membranes I. FTIR and XPS characterization of polyamide and coating layer chemistry, Desalination 242 (2009) 149-167.
[44] L.-Q. Li, Z.-M. Zhan, B.-Q. Huang, S.-M. Xue, C.-H. Ji, R.-Z. Wang, Y.-J. Tang, Z.-L. Xu, RO membrane fabricated via a facile modified heat-treating strategy for high-flux desalination, J. Membr. Sci. 614 (2020) 118498.
[45] Y.L. Liu, Y.Y. Zhao, X.M. Wang, X.H. Wen, X. Huang, Y.F.F. Xie, Effect of varying piperazine concentration and post-modification on prepared nanofiltration membranes in selectively rejecting organic micropollutants and salts, J. Membr. Sci. 582 (2019) 274-283.
[46] Q. Li, Z. Liao, X. Fang, J. Xie, L. Ni, D. Wang, J. Qi, X. Sun, L. Wang, J. Li, Tannic acid assisted interfacial polymerization based loose thin-film composite NF membrane for dye/salt separation, Desalination 479 (2020) 114343.
[47] Q. Shen, S.J. Xu, Z.Q. Dong, H.Z. Zhang, Z.L. Xu, C.Y. Tang, Polyethyleneimine modified carbohydrate doped thin film composite nanofiltration membrane for purification of drinking water, J. Membr. Sci. 610 (2020).
[48] W.R. Bowen, H.N.S. Yousef, Effect of salts on water viscosity in narrow membrane pores, J. Colloid Interface Sci. 264 (2003) 452-457.
[49] J.Q. Luo, Y.H. Wan, Effects of pH and salt on nanofiltration-a critical review, J. Membr. Sci. 438 (2013) 18-28.
[50] J. Gilron, N. Gara, O. Kedem, Experimental analysis of negative salt rejection in nanofiltration membranes, J. Membr. Sci. 185 (2001) 223-236.
[51] J.V. Nicolini, C.P. Borges, H.C. Ferraz, Selective rejection of ions and correlation with surface properties of nanofiltration membranes, Separ. Purif. Technol. 171 (2016) 238-247.
[52] B.Q. Huang, Y.J. Tang, Z.X. Zeng, Z.L. Xu, Microwave heating assistant preparation of high permselectivity polypiperazine-amide nanofiltration membrane during the interfacial polymerization process with low monomer concentration, J. Membr. Sci. 596 (2020).
[53] A.E. Yaroshchuk, Negative rejection of ions in pressure-driven membrane processes, Adv. Colloid

Interface Sci. 139 (2008) 150-173.
[54] D. Ren, X.T. Bi, T.Y. Liu, X.L. Wang, Oligo- ethylene- glycol based thin- film composite nanofiltration membranes for effective separation of mono-/di-valent anions, J. Mater. Chem. A. 7 (2019) 1849-1860.
[55] Y.-L. Ji, W.-J. Qian, Q.-F. An, S.-H. Huang, K.-R. Lee, C.-J. Gao, Mussel-inspired zwitterionic dopamine nanoparticles as building blocks for constructing salt selective nanocomposite membranes, J. Membr. Sci. 572 (2019) 140-151.
[56] S. Xiong, D.Y. Zhang, S. Mei, J. Liu, Y.S. Shi, Y. Wang, Thin film composite membranes containing intrinsic CD cavities in the selective layer, J. Membr. Sci. 551 (2018) 294-304.
[57] C. Wang, Z. Li, J. Chen, Z. Li, Y. Yin, L. Cao, Y. Zhong, H. Wu, Covalent organic framework modified polyamide nanofiltration membrane with enhanced performance for desalination, J. Membr. Sci. 523 (2017) 273-281.